PREDICTION OF NOISE REDUCTION BY AN ACTIVE FLAP OF A MODEL ROTOR

Yasutada Tanabe, Noboru Kobiki
e-mail: tan@chofu.jaxa.jp
JAXA (JAPAN)

Hideaki Sugawara
Ryoyu Systems, Co., Ltd. (JAPAN)

Abstract

The noise reduction by an active flap is predicted for a model rotor to be tested in JAXA. The elastic deformations of the blade are calculated based on the design blade structural properties. An analysis tool chain consisting of structural natural vibration mode analysis, CFD/CSD/Trim coupling analysis and noise prediction which are developed in-house is used. The BVI noise variation with the shaft angle is studied and where the maximum BVI noise observed is selected as the baseline test condition. The noise changes due to actuation of the flap at 2/rev with phase angle sweep is investigated. With amplitude of 3 deg, maximum noise reduction is observed at phase angle of 210 deg. These pre-test analysis results provided valuable guideline for the follow-on wind tunnel experiments.

1. INTRODUCTION

Noise has been regarded as one of the most serious problems for helicopter along with the cost and comfortableness. Operations are restricted in the urban area because of the noise concerns especially during night time which limits the utility of public service helicopters, such as emergency medical services (EMS) from the hospital based heli-pads. Noise from the helicopter sometime becomes a problem for the rescue activities on ground after a disastrous earthquake for example. Although quieter helicopters such as with NOTAR design are used more frequently for EMS, helicopters are still viewed as a noisy flying machine by most people. Revolutionary methods to reduce the helicopter noise remarkably are required and active control of the rotor blade is considered as one of the most promising approaches.

Various active control devices have been proposed and tested. Between them, active flap has been tested most extensively while other devices such as active tab and active twist are proposed with better effects or specific advantages. Several full-scale rotor blades with active flaps have been manufactured and tested in the wind-tunnels and during flights. Significant noise reduction capability has been reported especially during descent flight where the noise caused by the Blade-Vortex Interaction (BVI) is dominant. JAXA has been working on a full-scale active flap drive mechanisms and design of a full-sized blade installed with an active flap [1,2]. To demonstrated the noise reduction capability and obtain experimental data that can be used for validation of the rotor noise prediction tool, a model two-bladed rotor with active flap is built and wind tunnel testing is planned. This report will describe the design of the model rotor and part of the result of the pre-test predictions.

2. NUMERICAL APPROACHES

An analysis tool chain has been constructed at JAXA [3] as shown in Figure 1. In the first step, the natural frequencies and modes of the rotating blade is calculated based on the structural properties of the blade and the operating conditions of the rotor. A code named as *rMode* is developed to obtain the natural frequencies and modes required as inputs for CFD/CSD coupling analyses, which can also carry out the so-called fan-plot analysis and is useful for structural design of a blade to avoid vibrational resonance. The core of the multi-disciplinary analysis tool chain is the code named *rFlow3D/JANUS* which performs coupling CFD/CSD/Trim analyses based on a moving overlapped grid approach [4]. The *JANUS* code [5] combines an unstructured grid solver (*TAS-code*) [6] for the flowfield around the fuselage with the *rFlow3D* structured grid solvers for the blades and the background rectilinear grids. The deformation of a blade is described using the Ritz's mode decomposition method and is loosely coupled with the CFD solver, with the periodicity of the blade rotation presupposed. A numerically iterative solution to the Houbolt and Brooks' equation [7] based on coupled flapwise and chordwise bending and uncoupled torsion modes is found to improve the accuracy of the elastic deformations and more flexible to handle blade design changes, such as the

location of sectional center of gravity compared to the solutions based on full coupled mode shapes where the formulations are simpler [8]. Trim adjustment in the rotor controls is also rendered in the CSD routine in order to match up with the target thrust and moments. Finally, after a periodically converged solution of the flowfield together with the blade deformation is obtained, the noise generated by the rotor is then predicted based on the Ffowcs-Williams and Hawking's equations using the integral method in Farassat Formulation 1 [9] with the code named *rNoise*.

The airloads, elastic deformation and noise prediction accuracies are demonstrated based on HART-II test cases [10]. Details of the CFD methods utilized in rFlow3D can be found in ref.[11].

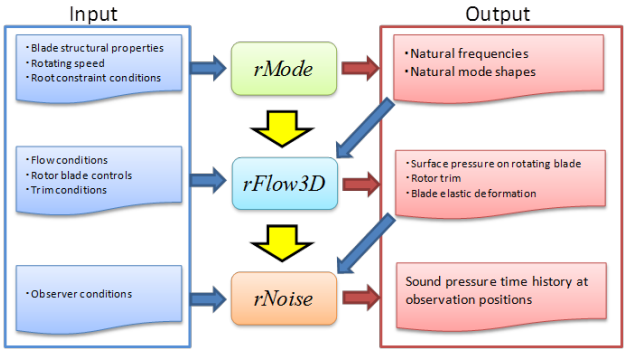

Figure 1: Analysis tool chain for helicopter aeroelasiticity and noise prediction

The converged periodic surface pressure data of one revolution are used to calculate the noise from the rotor. The code *rNoise* considers the elastic motions of the blade when generating the sound source cell position and directions. The sound pressure level for the BVI noise (BVISPL) is calculated based on the definition of ref.[12].

$$BVISPL = 20 \cdot \log\left(\sqrt{\sum_{i=6\times NBLD}^{40\times NBLD} p_i} \cdot \frac{1}{p_{ref}} \right)$$

3. ACTIVE FLAP MODEL ROTOR

The model rotor built in JAXA consists of two blades with a radius of 1.5m as shown in Figure 2. The active flap is intalled from 70% R to 80% R and a chord of 20% c. The design parameters is shown in Table 1.

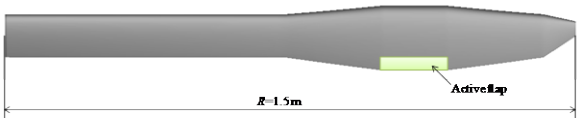

Figure 2: Planform of the model rotor blade with active flap

Table 1: Design parameter of the model blade

No. of blade	2
Blade radius, R	1.5 m
Chord length, c	0.1 m, 0.15 m (AF pos.)
Twist	-8
Airfoil	NACA23012
AF chord length	0.03 m (0.2c)
AF length	0.15 m (0.1R)
Rotor speed, Ω_0	133.3 rad/s

The natural frequencies of the rotor blade with change of rotating speed (the so-called Fan-plot) is calculted using rMode as shown in Figure 3. The structural properties are the design values and will be validated through ground test later on.

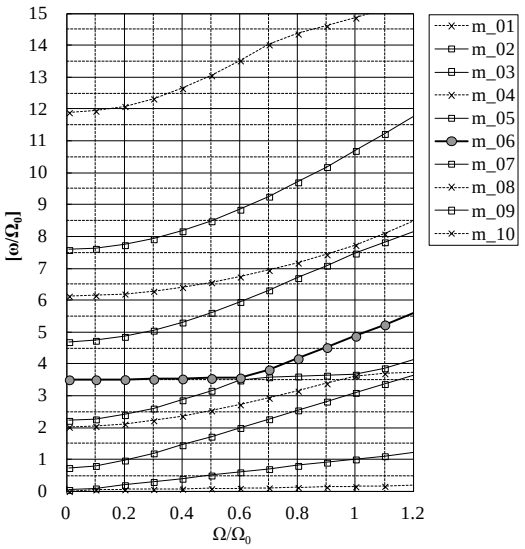

Figure 3: Fan-plot for JAXA model rotor blade with active flap

4. RESULTS AND DISCUSSIONS

Two layers of background grid have been used as shown in Figure 4. The blade grid size is 121 points in spanwise, 101 points in chordwise and 21 points in bodywise directions. The mesh size in bodywise direction is adjusted according to the resolution in inner background so that sufficient overlapping between the blade grid and inner background grid is secured taking account of the 7 points stencil of the current 4th order scheme adopted. Inclusion of the fuselage into the analysis may have minor influence on the noise results. At this stage, only the isolated rotor configuration is studied.

The noise observation positions are located on a plane underneath of the rotor with a vertical distance of 1R (namely, 1.5m) for this study as shown in Figure 5.

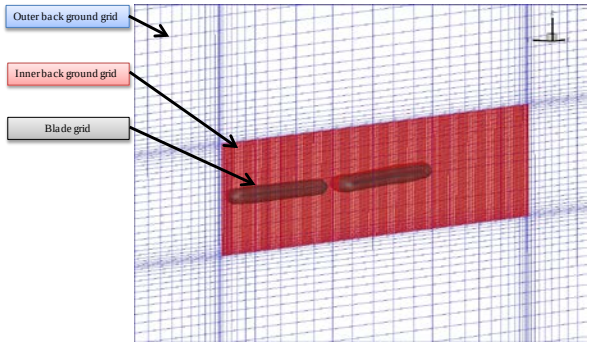

Figure 4: Overlapped grids

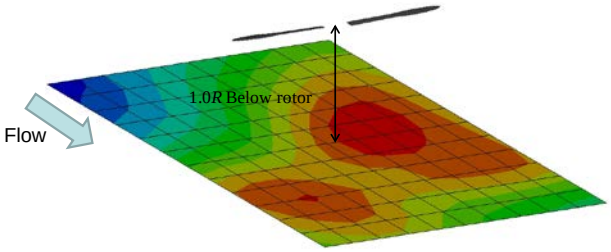

Figure 5: Noise observation plane

At first, the BVI noise variations due to rotor shaft angle change is investigated. The BVISPL contours are shown in Figure 6. It can be seen maximum BVI noise is observed at angle of 4 degrees. The maximum BVISPL is shown in Figure 7. The rotor blade is assumed to be rigid for the shaft angle sweep study. For the angles where BVISPL is high, also elastic blade computations are carried for comparison. As can be seen in Figure 7, elastic blade delivers lower maximum BVISPL comparably but the maximum BVISPL is at the same shaft angle. The difference between the rigid blade and elastic is within 0.2 dB. The elastic blade has a torsional deformation about -0.7 deg at the tip (see Figure 14, the baseline). That means a deeper negative twist and the airload is smaller at the tip area, so a weaker tip vortex and finally smaller BVI noise.

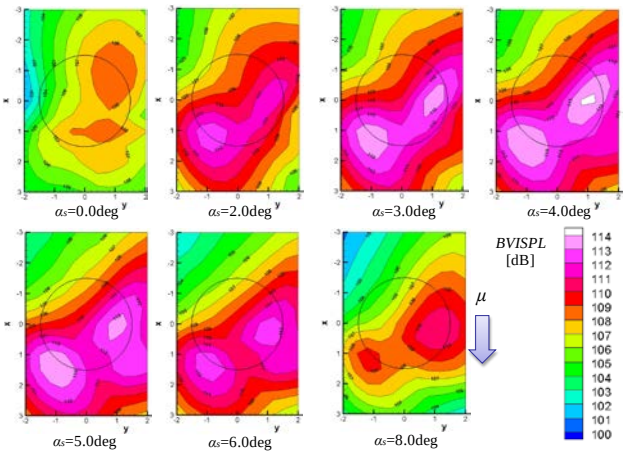

Figure 6: BVISPL Contours due to shaft angle change

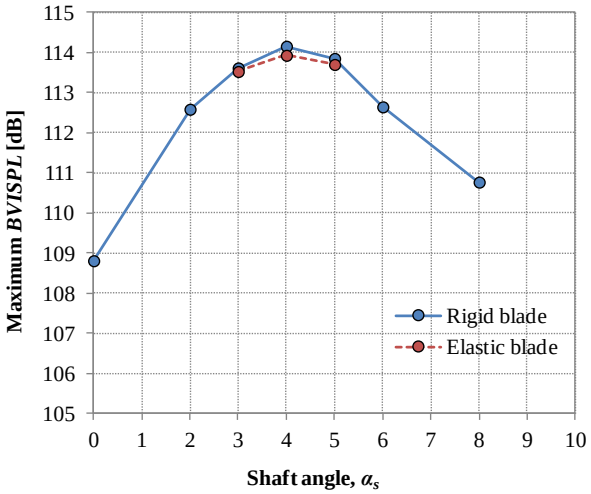

Figure 7: Maximum BVISPL due to shaft angle change at μ=0.15

At shaft angle of 4 degrees, the advance ratio is swept from 0.12 to 0.2. As shown in Figure 8, advance ratio of 0.15 has the maximum BVI noise level at this shaft angle. However, the difference from 0.14 to 0.16 is small, that means the BVISPL is not too sensitive to the wind speed change at this shaft angle condition.

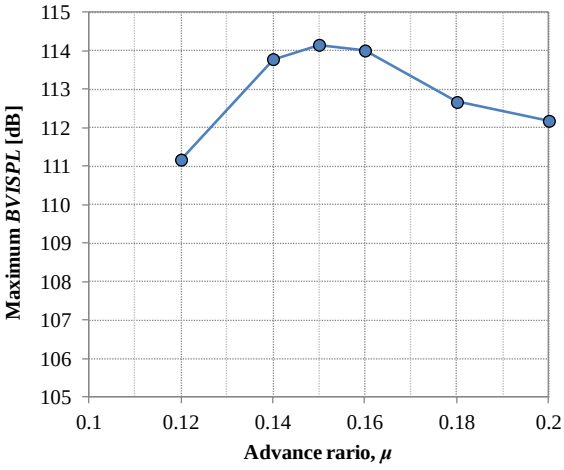

Figure 8: Maximum BVISPL due to advance ratio change at shaft angle of 4 deg

The active flap actuation is defined as shown in Figure 9. Flap down is defined as positive. The n is to be varied from 2 to 5 in the experiment. As a pre-test study, only n=2 is studied with the phase angle sweep from 0 deg to 330 deg at every 30 degree as shown in Table 2. The amplitude of the flap of 3 deg is assumed in this study. For the model rotor blade, the maximum amplitude depends on the frequency of the active flap actuation and the expected effect of BVI noise reduction may differ from this analysis

study.

$$\theta_{AF} = \theta_{AF0} + \sum_{n=1}^{N\max} \left(A_n \cdot \cos\left(n\Psi - \phi_n \right) \right)$$

Figure 9: Flap actuation definition

Table 2: Test cases of flap actuations

Flap amplitude, A_n	**3deg**
Flap frequency, n/rev	**2/rev**
Flap phase, f_n	**0～330**

The active flap is simulatled by deforming of the blade surface where the small gaps at each end are not simulated as shown in Figure 10. Dynamic deformation of the blade grid is performed automatically and the flap motion together with the blade motions and rotation are taken into account through the full unsteady formulations in the CFD routines [11].

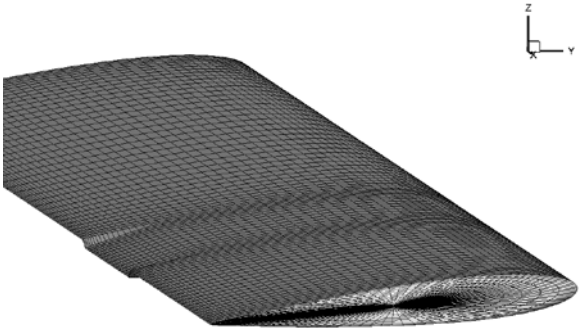

Figure 10: Blade surface deformation due to active flap

The BVI noise contours due to active flap actuation are shown in Figure 11. It can be observed that the noise contours are quite different and the active flap can control the BVI noise as expected. The maximum BVISPLs for each phase angle are shown in Figure 12. It can be seen that maximum BVISPL occurs at phase angle of 60 degrees and minimum BVISPL at 210 degrees. To understand the mechanism of BVI, these two phase angles will be compared in detail.

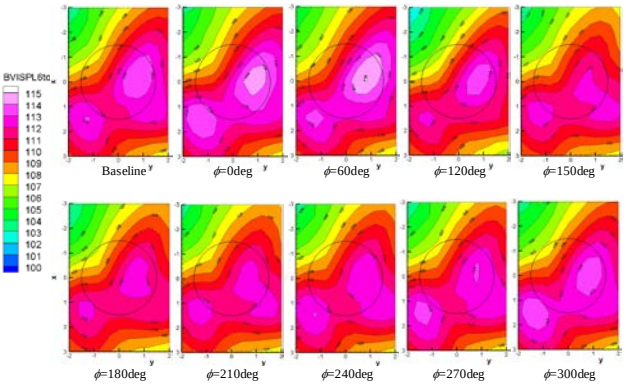

Figure 11: BVI noise contours due to active flap phase sweep at 2/rev with amplitude of 3 degrees

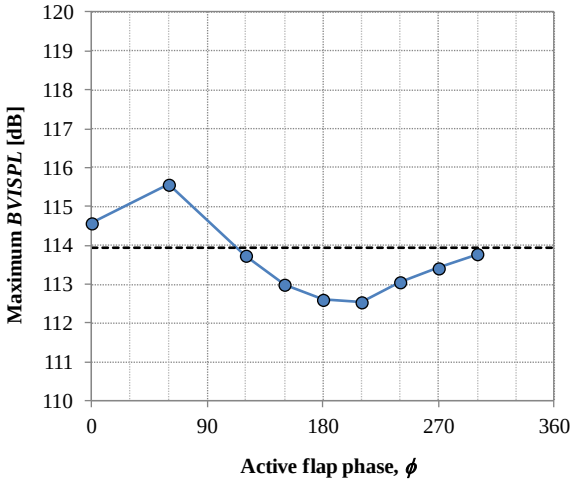

Figure 12: Maximum BVISPL due to phase sweep at 2/rev with amplitude of 3 degrees

As shown in Figure 13, the flap angle for these two phase angle are opposite to each other. The resulted torsional deformations are also opposite to each other where phase 210 deg has the largest negative torsional deformation at blade azimth angle of 130 deg which is in the upstream of the BVI occurence position in the rotor advancing side. From the vorticity contour in the Y plane crossing these two stations as shown in Figure 16, the tip vortex hits the blade near head-on at phase angle of 60 degrees. At phase angle of 210 degrees, a relatively large miss distance between the tip vortex and blade is observed, which corresponds to the minimum BVI noise level. Note that the tip vortex is above of the passing blade in Figure 16 (b). It can be expected that further larger elastic deformation may result in larger miss distance where blade pass through the tip vortices and further larger BVI noise reduction can be realized.

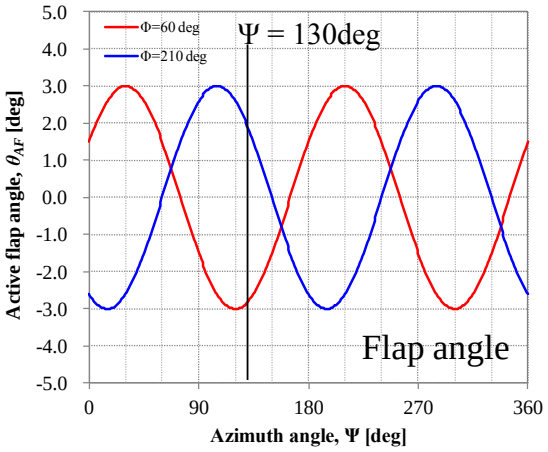

Figure 13: Active flap time history for phase angles 60 deg (max BVI) and 210 deg (min BVI)

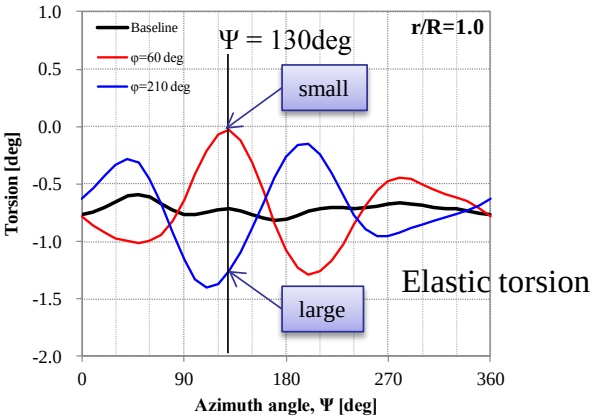

Figure 14: Torsional deformation time history for phase angles 60 deg (max BVI) and 210 deg (min BVI)

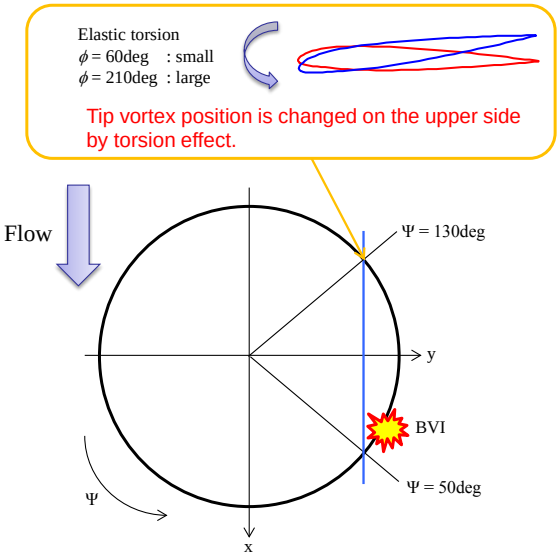

Figure 15: Sketch of the occurence of BVI

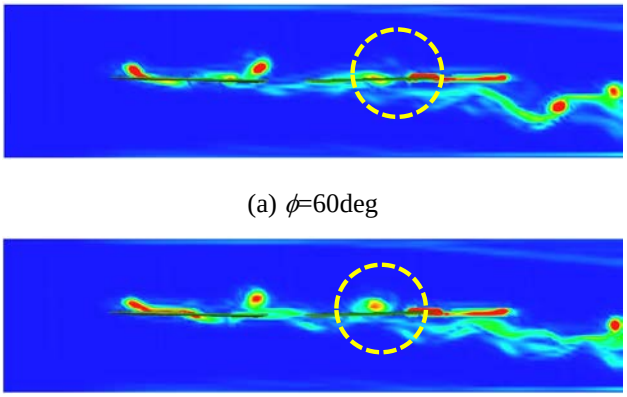

(a) ϕ=60deg

(b) ϕ=210deg

Figure 16: Vorticity contour for phase angles 60 deg (max BVI, head-on) and 210 deg (min BVI, large miss distane)

It must be noted that this pre-test analysis are based on the initial design blade structural properties and the active flap actuation amplitude may also differ from the follow-on wind tunnel testing. However, the predicted effects of shaft angle and the active flap phase angle sweep on the BVI noise levels provided valuable information for the planning of the wind tunnel testing and the pressure signals exacted from the simulation on the blade enables the construction of the BVI noise control laws beforehand of the measurement.

5. SUMMARY

The noise reduction by an active flap is predicted for a model rotor to be tested in JAXA. The elastic deformations of the blade are calculated based on the design blade structural properties. An analysis tool chain consisting of structural natural vibration mode analysis, CFD/CSD/Trim coupling analysis and noise prediction which are developed in-house is used.

The BVI noise variation with the shaft angle is studied at first. It is found that the maximum BVI noise is observed when shaft angle is 4 degrees. This is selected as the baseline test condition for further active control studies.

The noise changes due to actuation of the flap at 2/rev with phase angle sweep is investigated. With amplitude of 3 deg, maximum noise reduction is observed at phase angle of 210 deg.

These pre-test analysis results provided valuable guideline for the follow-on wind tunnel experiments.

REFERENCES

[1] Kobiki, N., Saito, S., Fukami, T., Komura, T., "Design and Performance Evaluation of Full

Scale On-board Active Flap System", 63rd Annual Forum of American Helicopter Society, Virginia Beach, VA, May 1-3, 2007.

[2] Kobiki, N., Saito, S., "Performance Evaluation of Full Scale On-board Active Flap System in Transonic Wind Tunnel", 64th Annual Forum of American Helicopter Society, Montreal, Canada, April 29-May 1, 2008.

[3] Tanabe, Y., Saito, S. and Sugawara, H., " Evaluation of Rotor Noise Reduction by Active Devices Using a CFD/CSD Coupling Analysis Tool Chain," 1st Asian Australian Rotorcraft Forum and Exhibition 2012, Busan, Korea, February 12-15, 2012.

[4] Tanabe, Y. and Saito, S., "A Simple CFD/CSD Loose Coupling Approach For Rotor Blade Aeroelasticity," 33rd European Rotorcraft Forum, Kazan, Russia, September 11-13, 2007. Also JAXA-RR-08-008E, March 2009.

[5] Tanabe, Y., Saito, S., Takayama, O., Sasaki, D. and Nakahashi, K., A New Hybrid Method of Overlapping Structured Grids Combined with Unstructured Fuselage Grids for Rotorcraft Analysis, 36th European Rotorcraft Forum, Paris, France, September 9-11, 2010.

[6] Nakahashi, K., Ito, Y. and Togashi, F., "Some challenges of realistic flow simulations by unstructured grid CFD", Int. J. for Numerical Methods in Fluids, Vol.43, pp.769-783, 2003.

[7] Houbolt, J.C. and Brooks, G.W., "Differential Equations of Motion for Combined Flapwise Bending, Chordwise Bending, and Torsion of Twisted Nonuniform Rotor Blades," NASA TN-3905, 1957.

[8] Tanabe, Y., Saito, S. and Sugawara, H., "Construction and Validation of an Analysis Tool Chain for Rotorcraft Active Noise Reduction," 38th European Rotorcraft Forum, Amsterdam, NL, September 4-7, 2012.

[9] Farassat, F., "Derivation of Formulation 1 and 1A of Farassat," NASA TM-2007-214853, 2007.

[10] Yu, Y.H., Tung, C., van der Wall, B., Pausder, H.-J., Burley, C., Brooks, T., Beaumier, P., Delrieux, Y., Mercker, E., & Pengel, K., "The HART-II Test: Rotor Wakes and Aeroacoustics with Higher-Harmonic Pitch Control (HHC) Inputs - The Joint German/French/Dutch/US Project -," AHS 58th Annual Forum, Montreal, Canada, June 11-13, 2002.

[11] Tanabe, Y. and Saito, S., "Significance of All-Speed Scheme in Application to Rotorcraft CFD Simulations," The 3rd International Basic Research Conference on Rotorcraft Technology, Nanjing, China. October, 2009.

[12] van der Wall, B.G., "2nd HHC Aeroacoustic Rotor Test (HART II) -Part I: Test Documentation -," DLR Institute Report IB 111-2003/31, 2003.